Published in IET Science, Measurement and Technology
Received on 14th January 2009
Revised on 25th October 2009
doi: 10.1049/iet-smt.2009.0003

ISSN 1751-8822

Adaptive complex unscented Kalman filter for frequency estimation of time-varying signals

P.K. Dash[1] S. Hasan[2] B.K. Panigrahi[3]
[1]Multidisciplinary Research Centre, SOA University, Bhubaneswar, India
[2]Silicon Institute of Technology, Bhubaneswar, India
[3]Indian Institute of Technology, New Delhi, India
E-mail: pkdash.india@gmail.com

Abstract: A simple and robust non-linear filter algorithm has been proposed in this study for estimating the frequency of a time-varying sinusoidal signal under high noise conditions. The real signal is first converted to an analytical signal and its complex state-space model is derived. An unscented complex Kalman filter (CUKF) is then obtained using the complex signal model and the error covariances along with the Kalman gain are updated iteratively. Also, the stability and the convergence characteristics of the proposed filter are presented for a single sinusoid embedded in noise. It has been shown that the proposed algorithm works efficiently for the estimation of abrupt changes in signal frequency under high noise conditions. To evaluate the performance of the proposed algorithm several computer simulation results of real-time and synthetic signals are presented. Further to improve the performance of the proposed filter in the presence of significant noise and distortions, the covariance matrices are tuned iteratively.

1 Introduction

The problem of estimating frequency and other parameters directly from measured discrete sinusoids in the presence of noise plays an important role in communication, control, instrument and power systems. Once the frequency of the signal is estimated, other parameters of the signal can accurately be estimated. Several methods are available in the literature on frequency estimation among which, the widely used once are: discrete Fourier transforms [1], least square technique [2], adaptive notch filter [3], multiple frequency tracker [4], high-order adaptive notch filters [5, 6], Newton type algorithms [7–9] and new variants of Kalman filter [10–13]. The notch filters in [2–4] track accurately the slow time-varying frequency of a sinusoid using linear filter approximation but fail to track sudden changes in system frequency during transient conditions. Further the filter in [5] uses different formulae and different tuning factors for tracking frequency for different non-stationary situations like linear frequency change, random walk frequency drift and step changes and thus is difficult to implement in practical situations where the signal frequencies change abruptly. The Newton type algorithms are computationally intensive and are likely to diverge for a wrong choice of the initial estimate.

Among the several numerical techniques described above, Kalman filters have attracted widespread attention, as they accurately estimate the amplitude, frequency and phase of a signal corrupted with high noise and harmonics. However, extended Kalman filter (EKF) has two well-known drawbacks; the first-order linearisation can introduce large errors in mean and covariance of the state vector, and costly Jacobean matrix calculation. The extended Kalman filters presented in the above references are able to track small linear changes in system frequency in high noise environment but fail to track sudden large step changes during transient conditions as in the case of several variants of adaptive notch filters. Recently, a relatively new non-linear derivative free filtering algorithm named unscented Kalman filter (UKF) is proposed [14–16] to decrease the linearisation errors by taking into consideration the second-order terms of Taylor series expansion. The UKF approximates the probability density resulting from the non-linear transformation of a random variable. It is implemented using a deterministic sampling approach to capture the mean and covariance estimates more accurately with a minimal set of sampling points.

Although the real versions of both EKF and UKF are used in many applications for tracking signal frequencies, the complex version of EKF is much simpler and direct as far as the frequency measurement is concerned and outperforms the real extended Kalman filter in terms of speed of convergence, accuracy and stability [17, 18]. Moreover, complex representations can make the measurement function the likelihood of linear formulation to reduce the influence of high-order terms. But the complex extended Kalman filter is still unable to track accurately the frequency in presence of harmonics and abrupt large transient disturbances. Hence to overcome the above-mentioned problems, a new complex UKF (CUKF) algorithm proposed in this paper. The CUKF uses an unscented transformation (UT) to a complex state-space model of the sinusoid and computes the covariances and the Kalman gain from the measurements corrupted with white noise. Further to improve its performance during large frequency changes, a self-tuning technique is used to update the model and measurement error covariances and this filter is named as adaptive unscented complex Kalman filter (ACUKF).

This paper is organised as follows; Section 2 presents a problem treated in this paper. Section 3 derives an algorithm of the proposed non-linear filter based on UKF. Section 4 gives the stability analysis of the proposed algorithm. Section 5 describes the ability of proposed algorithm through simulation results. Comparison with some of the existing algorithms is presented in this section to show the effectiveness of the proposed estimation technique. Section 6 concludes about the robustness of the algorithm.

2 Signal model

Consider a time-varying sinusoidal signal represented in discrete form as

$$z_k = A_k \cos(k\omega_k T_s + \phi_k) + v_k \tag{1}$$

where A_k, ω_k, ϕ_k and T_s are the amplitude, angular frequency, phase and sampling interval of the sinusoid, respectively; T_s is expressed as $T_s = 1/f_s$, $\omega_k = 2\pi f_k$, f_s and f_k are the sampling and fundamental frequency of the signal.

Since the observed signal is real, the development of a complex model requires a complex signal, and thus we use Hilbert transform [19] to convert the real signal z_k to an analytic signal of Gabor y_k as

$$y_k = A\mathrm{e}^{\mathrm{j}(k\omega T_s + \phi)} + \nu_k \tag{2}$$

The analytical signal $y(k)$ is modelled in the state space using the state variables x_{1k} and x_{2k} as

$$x_{1k} = \mathrm{e}^{\mathrm{j}(\omega T_s)} \tag{3}$$

$$x_{2k} = A_k \mathrm{e}^{\mathrm{j}(k\omega T_s + \phi)} \tag{4}$$

Note that the model can easily be extended to represent signals containing harmonics. Model equations (8) and (9) can be put in the general form as

$$\boldsymbol{x}_{k+1} = f(\boldsymbol{x}_k) + \boldsymbol{\eta}_k \tag{5}$$

and

$$y_k = h(\boldsymbol{x}_k) + v_k \tag{6}$$

where

$$f(\boldsymbol{x}_k) = [x_{1k} \quad x_{1k} \quad x_{2k}]^{\mathrm{T}} \tag{7}$$

and

$$h(\boldsymbol{x}_k) = [0 \quad 1]\begin{bmatrix} x_{1k} \\ x_{2k} \end{bmatrix} \tag{8}$$

The complex signal model used in equations (3)–(8) will be used in estimating the frequency of a time-varying sinusoid embedded in noise with low signal-to-noise ratio (SNR). The next section describes the UT and filtering algorithm.

3 Complex CUKF

As mentioned in the introduction the UKF is a powerful non-linear estimation technique and operates on the premise that it is easier to approximate a Gaussian distribution than it is to approximate an arbitrary non-linear function. Instead of linearising using Jacobean matrices the UKF evaluates the non-linear function with a minimal set of carefully chosen sampling points of $2L + 1$, sigma points (L is the state dimension) based on a square-root decomposition of the prior covariance [17]. These sigma points are propagated through the non-linearity, without approximation and a weighted mean and covariance is found. Like the EKF, the UKF uses a recursive algorithm that uses the system model, measurements and known statistics of the noise mixed with the signal. The posterior mean and covariances estimated from these sample points are accurate to the second order for any non-linearity.

Consider the non-linear system modelled by the discrete time state as in (7) and (8), where $\boldsymbol{x}_k \in R^L$ and $y_k \in R^P$ are the signal state and measurement, respectively. The non-linear mapping $f()$ is assumed to be continuously differentiable with respect to $\boldsymbol{x}_k$. Moreover $\boldsymbol{\eta}_k$ and v_k are uncorrelated zero mean Gaussian noise sequences with

$$E[\boldsymbol{\eta}_k \boldsymbol{\eta}_k^{*\mathrm{T}}] = Q_k = \begin{bmatrix} q_1 & 0 \\ 0 & q_2 \end{bmatrix}, \quad E[v_k v_k^{*\mathrm{T}}] = R_k, \quad E[\boldsymbol{\eta}_k v_k^{*\mathrm{T}}] = 0 \tag{9}$$

and the * sign indicates the complex conjugate of the quantity. The procedure for implementation of CUKF is as follows:

IET Sci. Meas. Technol., 2010, Vol. 4, Iss. 2, pp. 93–103
doi: 10.1049/iet-smt.2009.0003

Step-1: *Selection of sigma points*: Given an $L \times 1$ state vector $\hat{\boldsymbol{x}}_{k-1}$ at time step $k-1$ and state error covariance matrix $\hat{\boldsymbol{P}}_{k-1}$, compute a set of $2L+1$ sigma points as

$$\boldsymbol{\chi}_{k-1} = \left[\hat{\boldsymbol{x}}_{k-1} \quad \hat{\boldsymbol{x}}_{k-1} + \zeta\sqrt{\hat{\boldsymbol{P}}_{k-1}} \quad \hat{x}_{k-1} - \zeta\sqrt{\hat{\boldsymbol{P}}_{k-1}}\right] \quad (10)$$

where $\zeta = \sqrt{L+\lambda}$ and $\lambda = \alpha^2(L+\kappa) - L$, the parameter λ decides the spread of ith sigma point around $\hat{\boldsymbol{x}}_{k-1}$. For$\lambda > 0$, the points are scaled further from $\hat{\boldsymbol{x}}_{k-1}$ and when $\lambda < 0$, the points are scaled towards $\hat{\boldsymbol{x}}_{k-1}$. Further λ can be defined as a function of two parameters α and κ, where the constant α is a small constant lying between 0.0001 and 1 and can be used to control the amount of the higher-order non-linearities around $\hat{\boldsymbol{x}}_{k-1}$ which can be taken into account. The parameter κ is a secondary scaling parameter which is usually set to 0 or $3-L$ to ensure that the kurtosis of the sigma point distribution agrees with the kurtosis of a Gaussian distribution. The matrix $\zeta\hat{\boldsymbol{P}}_{k-1}$ is assumed positive definite and its square root can therefore be computed by using the Cholesky decomposition.

Step-2: *Transformation of sigma points through system function (time update)*: Each column of the sigma point matrix is propagated one step ahead through the dynamic function $f()$ of (5) to obtain the 'transformed sigma points' at time k

$$\boldsymbol{\chi}_{i,k} = f(\boldsymbol{\chi}_{i,k-1}), \quad i = 1, 2, \ldots 2L+1 \quad (11)$$

Step-3: Computation of prior state estimates: The prior state estimate $\hat{\boldsymbol{x}}_k^-$ and its corresponding covariance matrix $\hat{\boldsymbol{P}}_{k/k-1}$ are approximated by the weighted mean and covariance of the transformed sigma points as follows

$$\hat{\boldsymbol{x}}_k^- = \sum_{i=0}^{2L} W_i^{(m)}\boldsymbol{\chi}_{i,k} \quad (12)$$

$$\hat{\boldsymbol{P}}_{k/k-1} = \sum_{i=0}^{2L} W_i^{(c)}[\boldsymbol{\chi}_{i,k} - \hat{\boldsymbol{x}}_k^-][\boldsymbol{\chi}_{i,k} - \hat{\boldsymbol{x}}_k^-]^{*\mathrm{T}} + \boldsymbol{Q}_{k-1} \quad (13)$$

where $\boldsymbol{Q}_{k-1}$ is the process noise covariance matrix. The weights $W_i^{(m)}$ and $W_i^{(c)}$ are defined as

$$W_0^{(m)} = \frac{\lambda}{L+\lambda}, \quad W_i^{(m)} = \frac{\lambda}{2(L+\lambda)}, \quad W_{i+L}^{(m)} = \frac{1}{2(L+\lambda)} \quad (14)$$

$$W_0^{(c)} = \frac{\lambda}{(L+\lambda)} + (1-\alpha^2+\rho),$$
$$W_i^{(c)} = \frac{1}{2(L+\lambda)} + (1-\alpha^2+\rho), \quad (15)$$
$$W_{i+L}^{(c)} = \frac{1}{2(L+\lambda)}, \text{ and } \quad i = 1, \ldots, L$$

and ρ is another parameter used to incorporate prior knowledge of the higher-order moments of the state distribution. The optimal choice of this parameter for Gaussian distribution is 2.

Step-4: *Computation of predicted observation*: The predicted values for the manifest observations at time step k can be obtained as the weighted sum of the projection of transformed sigma points through measurement function h:

$$Y_{i,k} = h(\boldsymbol{\chi}_{i,k}) \quad (16)$$

$$\hat{y}_k^- = \sum_{i=0}^{2L} W_i^{(m)} Y_{i,k} \quad (17)$$

The posterior state estimate is computed as

$$\hat{\boldsymbol{x}}_k = \hat{\boldsymbol{x}}_k^- + \boldsymbol{K}_k(y_k - \hat{y}_k^-) \quad (18)$$

where $\boldsymbol{K}_k$ is the Kalman gain given by

$$\boldsymbol{K}_k = \boldsymbol{G}_k S_k^{-1} \quad (19)$$

where

$$\boldsymbol{G}_k = \sum_{i=0}^{2L} W_i^{(c)}[\boldsymbol{\chi}_{i,k} - \hat{\boldsymbol{x}}_k^-][Y_{i,k} - \hat{y}_k^-]^{*\mathrm{T}} \quad (20)$$

$$S_k = \sum_{i=0}^{2L} W_i^{(c)}[y_{i,k} - \hat{y}_k^-][Y_{i,k} - \hat{y}_k^-]^{*\mathrm{T}} + R_{k-1} \quad (21)$$

R_{k-1} is the measurement noise covariance. Then a posterior estimate of the error covariance matrix is given by

$$\hat{\boldsymbol{P}}_k = \hat{\boldsymbol{P}}_{k/k-1} - \boldsymbol{K}_k S_k \boldsymbol{K}_k^{*\mathrm{T}} \quad (22)$$

Like the UKF algorithm, the CUKF parameters $\boldsymbol{Q}_k$, R_k, α, ρ, κ are to be chosen by trial and error basis. The above implementation of CUKF has considered the model error covariance $\boldsymbol{Q}_k$ and measurement error covariance R_k are constants determined a priori. This paper also presents a self-tuning update procedure for model error covariance $\boldsymbol{Q}_k$ and the measurement error covariance R_k, in order to improve the filter adaptive capability and speed of the response.

The model error can be estimated at any instant k from (18) as

$$\boldsymbol{Z}_k = \hat{\boldsymbol{x}}_k - \hat{\boldsymbol{x}}_k^- = \boldsymbol{K}_k(y_k - \hat{y}_k^-) = [\psi_{1k}\psi_{2k}]^{\mathrm{T}} \quad (23)$$

As the model error is contributed by the white Gaussian noise, the calculated model error covariance matrix can be estimated from the above (23). Note that according to the number of states, which is two in the above CUKF, model $\boldsymbol{Z}_k$ takes different values, leading to different variance estimates given as

$$\hat{q}_{1k} = |\psi_{1k}|^2 \tag{24}$$

and

$$\hat{q}_{2k} = |\psi_{2k}|^2 \tag{25}$$

The model error covariance estimate can be taken as the average of both the terms and is given as

$$\hat{\boldsymbol{Q}}_k = \frac{1}{2}(\hat{q}_{1k} + \hat{q}_{2k}) \times \boldsymbol{I} \tag{26}$$

By taking the average any large value of either $\hat{q}_{1k}$ or $\hat{q}_{2k}$, which may be interpreted as a lack of accuracy of the whole model can be made adaptable. Similarly the measurement error covariance is estimated using innovation error $e_k = (y_k - \hat{y}_k^-)$, as

$$R_k = \lambda R_{k-1} + (1 - \lambda)|e_k||e_{k-1}| \tag{27}$$

where λ is forgetting factor and $0 \leq \lambda \leq 1$. In this way at every instant of time the model and the measurement error covariances are updated. The new values of model and measurement error covariances $\hat{\boldsymbol{Q}}_k$ and R_k are used to improve estimate of the state through iterative procedure. The initial setting of $\hat{\boldsymbol{Q}}_0 = 0 \times \boldsymbol{I}$ and $R_0 = 0$, and (26) and (27) are incorporated to the normal CUKF algorithm to make it adaptive ACUKF. Thus to verify the performance of the proposed filter, the internal behaviour of the filter like, Kalman gain, model and measurement error covariances of the filter is studied for tuned and untuned CUKF for a signal having abrupt change in frequency. The gain of the untuned filter settles to a fixed value even for change in signal parameter, where as the gain of the tuned filter adapts to the change in signal parameter, increasing the adaptive capability of the filter as shown in Fig. 1. Similarly Figs. 2 and 3 show the variation of the model and measurement error covariances of the filter. From the figures it is clear that the error covariances change with change in signal parameter changes to reduce the estimation error.

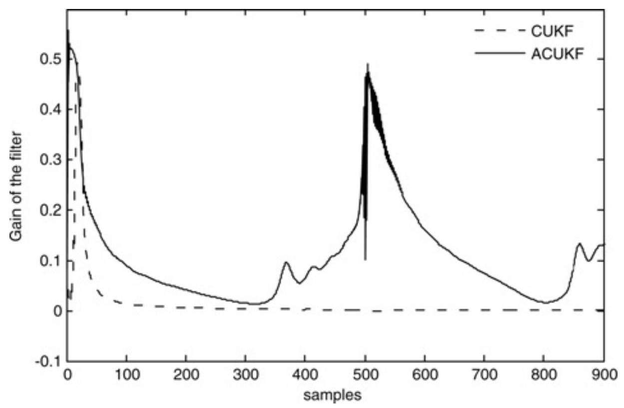

Figure 1 *Comparison of Kalman gain of the filter*

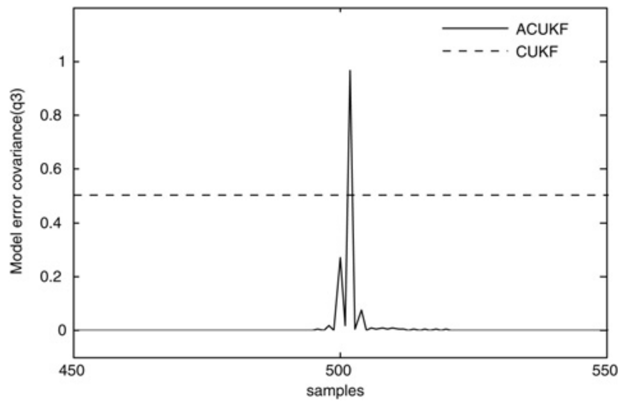

Figure 2 *Comparison of model error covariance the filter*

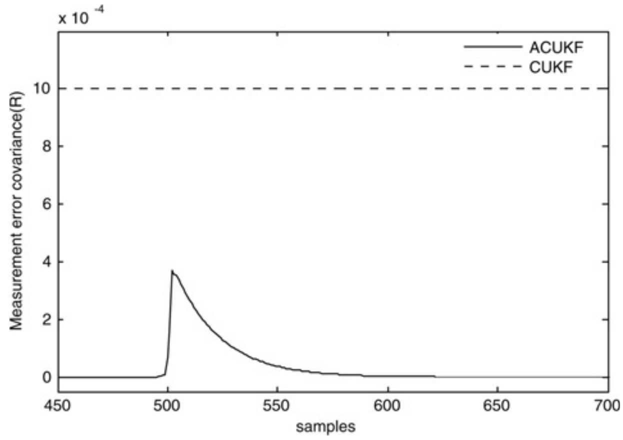

Figure 3 *Comparison of measurement error covariance of the filter*

4 Stability of the proposed non-linear filter

In this section, the stability of the proposed non-linear filter is derived using the unscented filter equations. It will be sufficient to show that the covariance matrix of estimation error converges to zero as time index k tends to infinity. Consider the non-linear discrete time system given in (5) and (6) representing the state and measurement vectors at time k, with $\boldsymbol{\eta}_k$ and v_k as the uncorrelated zero mean white noise having covariances $\boldsymbol{Q}_k$ and R_k, respectively. The estimation and prediction errors are defined by

$$\tilde{\boldsymbol{x}}_k = \boldsymbol{x}_k - \hat{\boldsymbol{x}}_k \tag{28}$$

$$\tilde{\boldsymbol{x}}_{k/k-1} = \boldsymbol{x}_k - \hat{\boldsymbol{x}}_k^- \tag{29}$$

Expanding $\boldsymbol{x}_k$ by a Taylor series about $\hat{\boldsymbol{x}}_{k-1}$ gives

$$\boldsymbol{x}_k = f(\hat{\boldsymbol{x}}_{k-1}) + \nabla f(\hat{\boldsymbol{x}}_{k-1})\tilde{\boldsymbol{x}}_{k-1} + \frac{1}{2}\nabla^2 f(\hat{\boldsymbol{x}}_{k-1})\tilde{\boldsymbol{x}}_{k-1}^2 + \cdots + \boldsymbol{\eta}_k \tag{30}$$

IET Sci. Meas. Technol., 2010, Vol. 4, Iss. 2, pp. 93–103
doi: 10.1049/iet-smt.2009.0003

Similarly expanding $\hat{\boldsymbol{x}}_k^-$ by Taylor series about $\hat{\boldsymbol{x}}_{k-1}$ gives

$$\begin{aligned}\hat{\boldsymbol{x}}_k^- &= \left(\frac{\lambda}{L+\lambda}\right) f(\hat{\boldsymbol{x}}_{k-1}) + \frac{\lambda}{2(L+\lambda)} \\ &\quad \times \sum_{i=1}^{L} f[\hat{\boldsymbol{x}}_{k-1} + (\gamma\sqrt{\boldsymbol{P}_{k-1}})_i] + \frac{\lambda}{2(L+\lambda)} \\ &\quad \times \sum_{i=L+1}^{2L} f[\hat{\boldsymbol{x}}_{k-1} - (\gamma\sqrt{\boldsymbol{P}_{k-1}})_{i-L}] \\ &= f(\hat{\boldsymbol{x}}_{k-1}) + \frac{1}{2}\nabla^2 f(\hat{\boldsymbol{x}}_{k-1})\boldsymbol{P}_{k-1} + \cdots\end{aligned} \tag{31}$$

Substituting (30) and (31) into (29) gives an approximate equation

$$\tilde{\boldsymbol{x}}_{k/k-1} \simeq \boldsymbol{F}_k \tilde{\boldsymbol{x}}_{k-1} + \boldsymbol{\eta}_k \tag{32}$$

where

$$\boldsymbol{F}_k = \left(\left.\frac{\partial f(x)}{\partial x}\right|_{x=\hat{x}_{k-1}} \right) = \begin{bmatrix} 1 & 0 \\ \hat{x}_{2\,k-1} & \hat{x}_{1\,k-1} \end{bmatrix} \tag{33}$$

In the above equation only the first term is taken, hence we use an unknown instrumental matrix $\boldsymbol{\beta}_k = \mathrm{diag}(\beta_{1k}, \beta_{2k}, \ldots, \beta_{Mk})$ to describe the prediction error without approximation, similar formulation has been used in [16] and is given by

$$\tilde{\boldsymbol{x}}_{k/k-1} = \boldsymbol{\beta}_k \boldsymbol{F}_k \tilde{\boldsymbol{x}}_{k-1} + \boldsymbol{\eta}_k \tag{34}$$

But in the proposed adaptive algorithm, the predicted covariance matrix is calculated as

$$\hat{\boldsymbol{P}}_{k/k-1} = \sum_{i=0}^{2L} W_i^{(c)} [\boldsymbol{\chi}_{i,k} - \hat{\boldsymbol{x}}_k^-][\boldsymbol{\chi}_{i,k} - \hat{\boldsymbol{x}}_k^-]^{*\mathrm{T}} + \hat{\boldsymbol{Q}}_{k-1} \tag{35}$$

where $\hat{\boldsymbol{Q}}_{k-1}$ is a positive definite matrix introduced in the calculation so that the stability of the filter will be improved, and let the real prediction error covariance matrix is given by

$$\hat{\boldsymbol{P}}_{k/k-1} = \begin{bmatrix} \hat{\sigma}^2_{k/k-1(1)} & \gamma_{k/k-1} \\ \gamma^*_{k/k-1} & \hat{\sigma}^2_{k/k-1(2)} \end{bmatrix} \tag{36}$$

where $\hat{\sigma}^2_{k/k-1}()$ and $\gamma_{k/k-1}$ represents the diagonal and off diagonal elements of $\hat{\boldsymbol{P}}_{k/k-1}$, respectively, and the real covariance matrix calculated taking the expectation yields

$$\begin{aligned}\hat{\boldsymbol{P}}_{k/k-1} &= E[\tilde{\boldsymbol{x}}_{k/k-1}\tilde{\boldsymbol{x}}^{*\mathrm{T}}_{k/k-1}] \\ &= E[(\boldsymbol{\beta}_k\boldsymbol{F}_k\tilde{\boldsymbol{x}}_{k-1} + \boldsymbol{\eta}_k)(\boldsymbol{\beta}_k\boldsymbol{F}_k\tilde{\boldsymbol{x}}_{k-1} + \boldsymbol{\eta}_k)^{*\mathrm{T}}] \\ &= \boldsymbol{\beta}_k\boldsymbol{F}_k\hat{P}_{k-1}\boldsymbol{\beta}_k^{*\mathrm{T}}\boldsymbol{F}_k^{*\mathrm{T}} + \hat{\boldsymbol{Q}}_{k-1}\end{aligned} \tag{37}$$

see (38)

Hence comparing (36) and (38) we obtain

$$\hat{\sigma}^2_{k/k-1}(1) = \beta_1^2\hat{\sigma}^2_{k-1}(1) + \hat{q}_{1\,k-1} \tag{39}$$

$$\gamma_{k/k-1} = \beta_1\beta_2(\hat{\sigma}^2_{k/k-1}(1)\hat{x}^*_{2\,k-1} + \gamma_{k-1}\hat{x}^*_{1\,k-1}) \tag{40}$$

$$\begin{aligned}\hat{\sigma}^2_{k/k-1}(2) &= \beta_1^*\beta_2(\hat{\sigma}^2_{k-1}(1)|\hat{x}_{2\,k-1}|^2 + \gamma^*_{k-1}\hat{x}_{1\,k-1}\hat{x}^*_{2\,k-1}) \\ &\quad + \beta_2^2(\gamma_{k-1}\hat{x}^*_{1\,k-1}\hat{x}_{2\,k-1} + \hat{\sigma}^2_{k-1}(2)|\hat{x}_{1\,k-1}|^2) + \hat{q}_{2\,k-1}\end{aligned} \tag{41}$$

As we know from the algorithm of CUKF

$$\hat{\boldsymbol{P}}_{k/k} = \hat{\boldsymbol{P}}_{k/k-1} - \boldsymbol{K}_k\boldsymbol{H}_k\hat{\boldsymbol{P}}_{k/k-1} \tag{42}$$

and the Kalman gain is given by

$$\boldsymbol{K}_k = (\hat{\boldsymbol{P}}_{k/k-1}\boldsymbol{H}_k^{*\mathrm{T}})(\boldsymbol{H}_k\hat{\boldsymbol{P}}_{k/k-1}\boldsymbol{H}_k^{*\mathrm{T}} + R_{k-1})^{-1} \tag{43}$$

$$\begin{aligned}\boldsymbol{K}_k &= \begin{bmatrix} \gamma_{k/k-1} \\ \hat{\sigma}^2_{k/k-1}(2) \end{bmatrix} \\ &\quad \times \left[[0 \quad 1] \begin{bmatrix} \hat{\sigma}^2_{k/k-1}(1) & \gamma_{k/k-1} \\ \gamma^*_{k/k-1} & \hat{\sigma}^2_{k/k-1}(2) \end{bmatrix} \begin{bmatrix} 0 \\ 1 \end{bmatrix} + R_{k-1} \right]^{-1} \\ &= \begin{bmatrix} \gamma_{k/k-1} \\ \hat{\sigma}^2_{k/k-1}(2) \end{bmatrix} [\hat{\sigma}^2_{k/k-1}(2) + R_{k-1}]^{-1} \\ &= \varepsilon_k^2 \begin{bmatrix} \gamma_{k/k-1} \\ \hat{\sigma}^2_{k/k-1}(2) \end{bmatrix}\end{aligned} \tag{44}$$

where

$$\varepsilon_k^2 = \frac{1}{\hat{\sigma}^2_{k/k-1}(2) + R_{k-1}} \tag{45}$$

$$\begin{aligned} &= \begin{bmatrix} \beta_1 & 0 \\ 0 & \beta_2 \end{bmatrix} \begin{bmatrix} 1 & 0 \\ \hat{x}_{2k-1} & \hat{x}_{1k-1} \end{bmatrix} \begin{bmatrix} \hat{\sigma}^2_{k-1(1)} & \gamma_{k-1} \\ \gamma^*_{k-1} & \hat{\sigma}^2_{k-1(2)} \end{bmatrix} \begin{bmatrix} \beta_1^* & 0 \\ 0 & \beta_2^* \end{bmatrix} \begin{bmatrix} 1 & \hat{x}^*_{2k-1} \\ 0 & \hat{x}^*_{1k-1} \end{bmatrix} + \hat{Q}_{k-1} \\ &= \begin{bmatrix} \beta_1^2\hat{\sigma}^2_{k-1}(1) & \beta_1^2\hat{\sigma}^2_{k-1}(1)\hat{x}^*_{2k-1} + \beta_1\beta_2^*\gamma_{k-1}\hat{x}^*_{1k-1} \\ \beta_1^*\beta_2\hat{\sigma}^2_{k-1}(1)\hat{x}_{2k-1} + \beta_1^*\beta_2\gamma^*_{k-1}\hat{x}_{1k-1} & \beta_1^*\beta_2(\hat{\sigma}^2_{k-1}(1)\hat{x}_{2k-1}\hat{x}^*_{2k-1} + \gamma^*_{k-1}\hat{x}_{1k-1}\hat{x}^*_{2k-1}) \\ & +\beta_2^2(\gamma_{k-1}\hat{x}_{2k-1}\hat{x}^*_{1k-1} + \hat{\sigma}^2_{k-1}(2)\hat{x}_{1k-1}\hat{x}^*_{1k-1}) \end{bmatrix} + \hat{Q}_{k-1} \end{aligned} \tag{38}$$

doi: 10.1049/iet-smt.2009.0003

Using above equations, the error covariance matrix becomes (see (46))

Hence

$$\hat{\sigma}^2_{k/k}(1) = \hat{\sigma}^2_{k/k-1}(1) - \varepsilon^2_k|\gamma_{k/k-1}|^2 \tag{47}$$

$$\gamma_{k/k} = \gamma_{k/k-1} - \varepsilon^2_k\gamma_{k/k-1}\sigma^2_{k/k-1}(2) \tag{48}$$

$$\hat{\sigma}^2_{k/k}(2) = \hat{\sigma}^2_{k/k-1}(2) - \varepsilon^2_k\hat{\sigma}^4_{k/k-1}(2) \tag{49}$$

Now replacing $\hat{\sigma}^2_{k/k-1}(1)$, $\hat{\sigma}^2_{k/k-1}(2)$, $\gamma_{k/k-1}$ with its relation to time $k-1$ we obtain

$$\begin{aligned}\hat{\sigma}^2_{k/k}(1) &= \beta^2_1\hat{\sigma}^2_{k-1}(1) + \hat{q}_{1k-1} - \varepsilon^2_k|\gamma_{k/k-1}|^2 = \hat{\sigma}^2_{k/k}(1)\\ &\quad - \beta^2_1\hat{\sigma}^2_{k-1}(1) = \hat{q}_{1k-1} - \varepsilon^2_k|\gamma_{k/k-1}|^2\end{aligned} \tag{50}$$

Further ε^2_k is approximately proportional to $1/R_{k-1}$ as given in (45) and both $\hat{q}_{1k-1}$ and R_{k-1} decrease as k increases resulting in the condition $|\hat{q}_{1k-1}| < \varepsilon^2_k|\gamma_{k/k-1}|^2$. Thus it can be observed that the variance in (50) continues to decrease as k increases, and at the equilibrium point $\gamma_{k/k-1} = 0$ and $\hat{q}_{1k-1}$ converges to a very small value, which is almost equal to 0. Thus from (48) it is clear that $\gamma_{k/k}$ also will tend to zero. Following the similar process as for $\hat{\sigma}^2_{k/k}(1)$ we can verify that $\hat{\sigma}^2_{k/k}(2)$ also converges to zero. Hence the estimation error covariance converges to zero as k becomes very large or tends to infinity.

Further $\boldsymbol{\beta}_k$ in (34) is an unknown instrumental diagonal matrix chosen for evaluating the error introduced by the UT and stability of the ACUKF algorithm does not depend on the magnitude of $\boldsymbol{\beta}_k$, whose value is set to $\boldsymbol{\beta}_k = \boldsymbol{I}$ $(\beta_1 = 1,\ \beta_2 = 1)$. To ensure the stability of ACUKF, the matrix $\hat{\boldsymbol{Q}}_{k-1}$ needs to be positive definite. It can be seen from (26) that $\hat{\boldsymbol{Q}}_{k-1}$ is a small positive quantity. If $\hat{\boldsymbol{Q}}_{k-1}$ is sufficiently large, then ACUKF can tolerate high-order error introduced during the UT by enlarging the noise covariance matrix. On the other hand, when the matrix $\hat{\boldsymbol{Q}}_{k-1}$ is enlarged, stability of the ACUKF will be improved, but the precision may be decreased.

5 Simulation results and discussion

Different cases of time varying frequency change are tested using the proposed approach and different filters. Test-1 analyses different types of major power signal variation problems, such as sudden frequency change and harmonic distortion, using simulated waveforms and MATLAB software package; Test-2 analyses distorted signals generated using an experimental setup. The chosen sampling rate is 1 kHz, for Test-1 and 2.3 kHz for Test-2, and the frequency is normalised with respect to a base frequency.

5.1 TEST- 1

In this test several case studies have been undertaken which are given below.

Case 1: The effectiveness of the proposed algorithm adaptive CUKF with complex-EKF and UKF has been demonstrated considering the non-stationary signal under different levels of noise, the SNR is varied from 60 to 10 dB. The non-linear signal considered is given by

$$y_k = A_k\cos(k\omega_k T_s + \phi_k) + v_k \tag{51}$$

where A_k, ω_k and ϕ_k are the amplitude, frequency and phase of the signal, respectively, and v_k is Gaussian noise with zero mean. For tracking a time varying power signal of 50 Hz frequency, the sampling frequency is chosen as 1.0 kHz and the CUKF parameters $\boldsymbol{Q}_k$, R_k, α, β and κ need to be initialised. Here β and κ are chosen as $\beta = 2$ and $\kappa = 0$ and $\alpha = 0.5$, $\boldsymbol{Q}_k = q_k\boldsymbol{I}_{2\times2}$, where I is a unit matrix and $q_k = 0.5$, and $R_k = 0.05$. Since the non-linear model used in the proposed algorithm uses two states for modelling, the value of L is set equal to 2, and thus the number of sigma points for this estimation is $2L+1$, that is, 5 and the augmented state vector $\boldsymbol{\chi}_{k-1}$ is a 2×5 matrix. The frequency of the time varying signal is given by

$$f_k = 50\,\text{Hz},\ \text{for } 0 \le k \le 500,\ \text{and} f_k = 70\ \text{Hz},\ \text{for } k \ge 500 \tag{52}$$

$$\begin{aligned}\hat{P}_{k/k} &= \begin{bmatrix}\hat{\sigma}^2_{k/k-1}(1) & \gamma_{k/k-1}\\ \gamma^*_{k/k-1} & \hat{\sigma}^2_{k/k-1}(2)\end{bmatrix} - \varepsilon^2_k\begin{bmatrix}\gamma_{k/k-1}\\ \hat{\sigma}^2_{k/k-1}(2)\end{bmatrix}\begin{bmatrix}0 & 1\end{bmatrix}\begin{bmatrix}\hat{\sigma}^2_{k/k-1}(1) & \gamma_{k/k-1}\\ \gamma^*_{k/k-1} & \hat{\sigma}^2_{k/k-1}(2)\end{bmatrix}\\ &= \begin{bmatrix}\hat{\sigma}^2_{k/k-1}(1) & \gamma_{k/k-1}\\ \gamma^*_{k/k-1} & \hat{\sigma}^2_{k/k-1}(2)\end{bmatrix} - \varepsilon^2_k\begin{bmatrix}\gamma_{k/k-1}\gamma^*_{k/k-1} & \gamma_{k/k-1}\hat{\sigma}^2_{k/k-1}(2)\\ \hat{\sigma}^2_{k/k-1}(2)\gamma^*_{k/k-1} & \hat{\sigma}^2_{k/k-1}(2)\hat{\sigma}^2_{k/k-1}(2)\end{bmatrix}\\ &= \begin{bmatrix}\hat{\sigma}^2_{k/k-1}(1) - \varepsilon^2_k|\gamma_{k/k-1}|^2 & \gamma_{k/k-1} - \varepsilon^2_k\gamma_{k/k-1}\hat{\sigma}^2_{k/k-1}(2)\\ \gamma^*_{k/k-1} - \varepsilon^2_k\hat{\sigma}^2_{k/k-1}(2)\gamma^*_{k/k-1} & \hat{\sigma}^2_{k/k-1}(2) - \varepsilon^2_k\hat{\sigma}^4_{k/k-1}(2)\end{bmatrix}\end{aligned} \tag{46}$$

doi: 10.1049/iet-smt.2009.0003

The SNR of the signal is varied from 60, 30, 20 and 10 dB, respectively. The experiment was repeated 100 times. The frequency tracking ability of different algorithms is summarised in Table 1, which shows a comparison between the UKF, CEKF, CUKF and adaptive CUKF for the signal model shown in (51). Fig. 4 shows the frequency tracking performance of different algorithms. It is clear from the figure that UKF is unable to track large step change in frequency even at 30 dB white Gaussian noise as compared to ACUKF. The performance of ACUKF is even better than the CEKF.

Case 2: The non-linear signal considered in this case is the same one given in (51), and the time varying frequency considered is given by

$$f_k = 50\,\text{Hz, for } 0 \le k \le 500, \text{ and } f_k = 52\,\text{Hz, for } k \ge 500 \qquad (53)$$

The SNR of the signal is then varied in a similar way from 60 to 10 dB as in case 1. The experiment was repeated 100 times, and the frequency tracking performance of the filters is summarised in Table 2. Fig. 5 shows that for small-step frequency variation both UKF and adaptive IIR systems (AIS) (adaptive infinite impulse response (IIR) structure) can track frequency more or less accurately as in the case of=ACUKF. It is clear from the figure that although UKF and AIS can track small variations in frequency, the performance of proposed ACUKF filter is better.

Table 1 MSE over 100 independent runs

Algorithm	60 dB	30 dB	20 dB	10 dB
UKF	0.0986	0.213	0.32	0.511
CEKF	0.0073	0.051	0.089	0.257
CUKF	0.0052	0.028	0.076	0.208
ACUKF	0.0011	0.0163	0.051	0.121

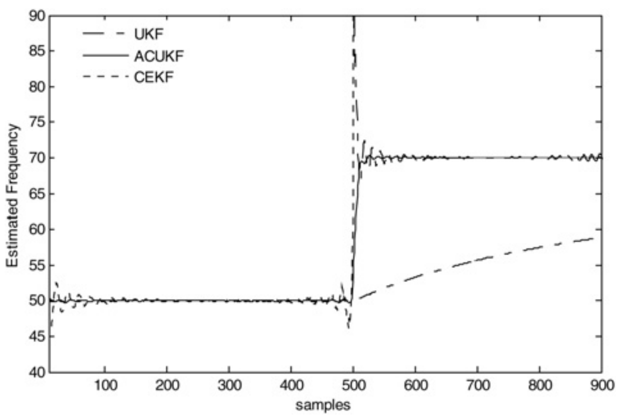

Figure 4 *Frequency tracked with different algorithms at SNR 30 dB*

Table 2 Mean of MSE over 100 independent runs

Algorithm	60 dB	30 dB	20 dB	10 dB
AIS	0.0583	0.0971	0.212	0.473
UKF	0.0173	0.0192	0.187	0.401
CUKF	0.00093	0.0083	0.066	0.157
ACUKF	0.00075	0.0016	0.028	0.143

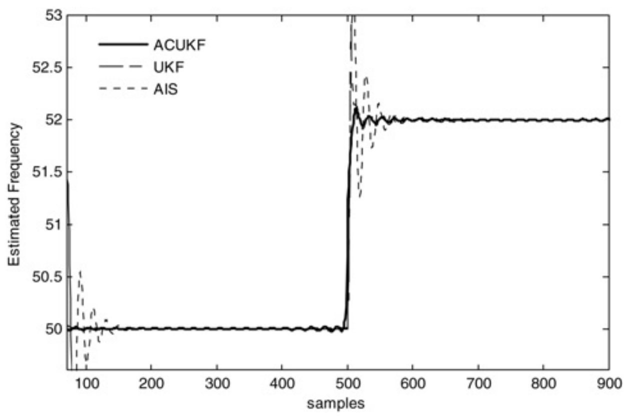

Figure 5 *Frequency tracked with different algorithms at SNR 30 dB*

Case 3: A similar analysis as in case 2 is repeated for a frequency variation of

$$f_k = 45\,\text{Hz}, \quad \text{for } 0 \le k \le 500, \text{ and}$$
$$f_k = 55\,\text{Hz}, \quad \text{for } k \ge 500 \qquad (54)$$

In this case the performance of AIS and ACUKF is compared for different SNR. Fig. 6 shows that for a

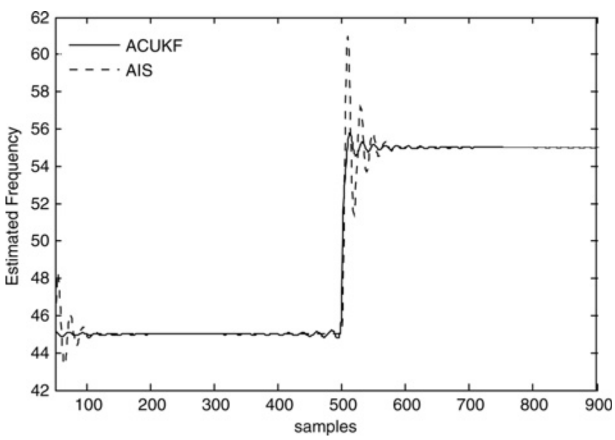

Figure 6 *Frequency tracked with different algorithms at SNR 10 dB*

step frequency variation AIS algorithm can track frequency, but it takes large setting time compared to ACUKF.

Case 4: The signal considered in this case is same as given in (51). The frequency of the signal is varied linearly with a constant increment and is given as follows.

For

$$k \le k_s, \quad f_k = f_0, \quad k_s < k \le k_F, \quad f_k = f_0 + \Delta f, \quad \text{and} \quad k > k_F f_k = f_1 \tag{55}$$

where $f_0 = 45\,\text{Hz}$, $f_1 = 55$, and $\Delta f = (k - k_s)(f_1 - f_0)/T_s(k_F - k_s)$ The performance of different algorithms for high noise condition is presented in Fig. 7. It is clear from the figure that AIS does not perform well at high noise condition even for linear frequency variation. On the other hand although CEKF is able to track the frequency under high noise condition, it takes more time to converge to the true value as compared to the proposed ACUKF.

Case 5: The non-linear signal considered in this case is the same one as in (51). The fundamental frequency of the signal is modulated by a small frequency component. Fig. 8 shows the modulated frequency tracking performance of ACUKF, CUKF and UKF under high noise condition of SNR = 10 dB. From the figure it is clear that the ACUKF and CUKF can easily track the modulated frequency compared to UKF.

Case 6: In this case 10% third harmonic, 1% fifth harmonic and 0.5% seventh harmonic are added to the signal considered in case 1. Since harmonics are not considered in the signal model, the performance of the proposed filter is expected to deteriorate. Fig. 9 shows the frequency tracking performance of ACUKF in the presence of unmodelled harmonics. It is observed from Fig. 9 that the

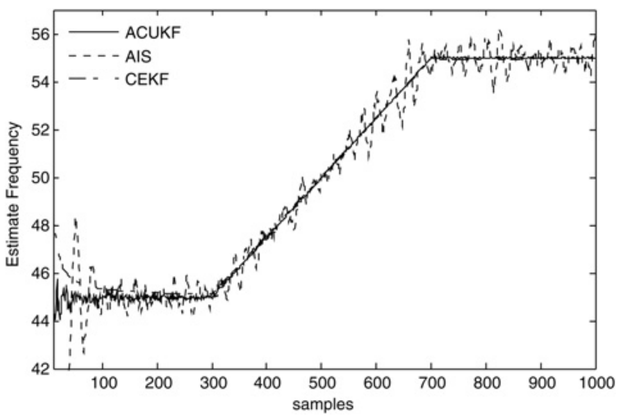

Figure 7 *Ramp Frequency tracked with different algorithms at SNR 10 dB*

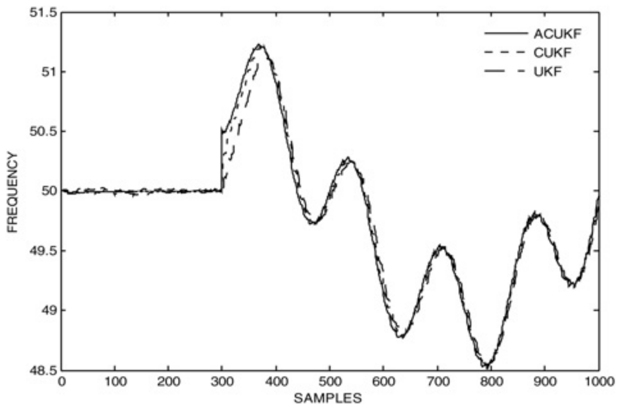

Figure 8 *Modulated Frequency tracked with different algorithms at SNR 10 dB*

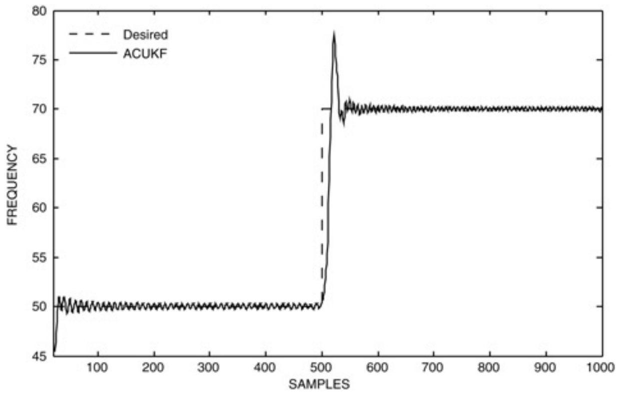

Figure 9 *Performance of the algorithm in presence of harmonics as noise: actual (dotted), estimated (solid)*

presence of harmonic hardly affects the fundamental frequency estimation. However, if the magnitudes of harmonic components are significant, the performance of ACUKF will deteriorate, if the signal model does not include them.

5.2 TEST-2

Case 7: Experimental test data are generated using practical setup, as shown in Figs. 10*a* and *b*, and then the proposed method is applied to the acquired signals. The sampling rate is chosen as 2.3 kHz. The load is fed from a 3 kVA, 230:230 single-phase transformer, and signals are obtained by switching on and switching off the load, respectively. The data samples are collected by stepping down the load voltage to 12 V and then converted to digital signal by data acquisition card (DAC) and collected in the PC using the program written in 'C'. The signal generated is a time-varying signal where frequency of the signal changes from 10 to 18 Hz then comes back to 10 Hz. The frequency tracking performance is summarised in Table 3 for

doi: 10.1049/iet-smt.2009.0003

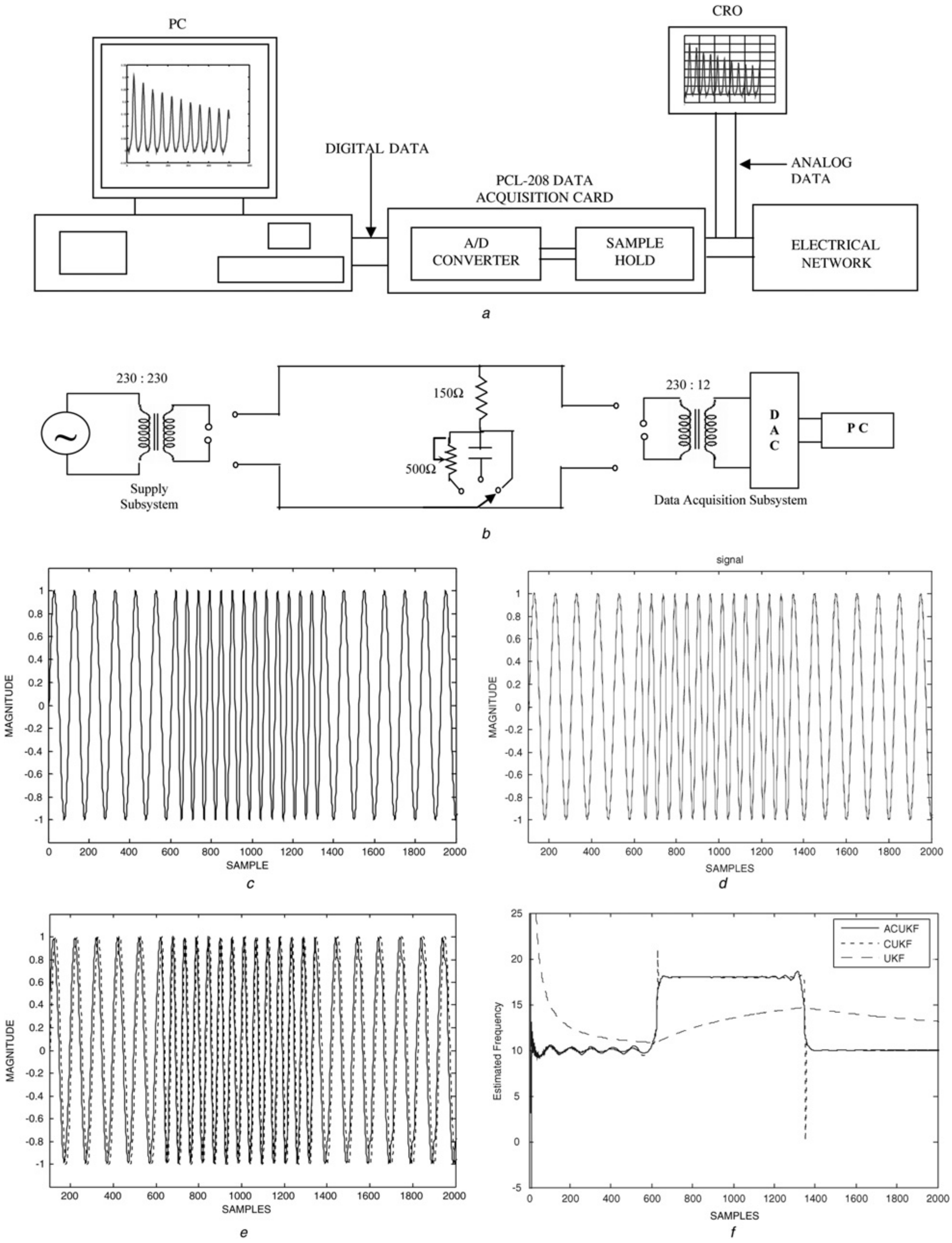

Figure 10 *Real-time signal tracking during frequency step-up*

a Experimental setup
b Waveform simulator subsystem
c Real-time signal
d Real-time signal tracked using CUKF algorithm: actual (dotted), estimated (solid)
e Real-time signal tracked using UKF algorithm; actual (dotted), estimated (solid)
f Real-time signal frequency tracked with different algorithms

Table 3 Mean of MSE over 100 independent runs

Algorithm	60 dB	30 dB	20 dB	10 dB
UKF	0.068	0.081	0.121	0.231
CUKF	0.0066	0.033	0.092	0.211
ACUKF	0.0023	0.0263	0.085	0.205

Table 4 Mean of MSE over 100 independent runs

Algorithm	60 dB	30 dB	20 dB	10 dB
UKF	0.082	0.093	0.127	0.242
CUKF	0.0054	0.045	0.108	0.21
ACUKF	0.0026	0.031	0.095	0.201

different algorithms. Fig. 10*c* shows the real-time signal obtained from the experimental setup. Figs. 10*d* and *e* show the signal tracking performance of the CUKF and EKF algorithms, respectively. Fig. 10*f* shows the comparative frequency tracking performance of ACUKF, CUKF and UKF algorithms. Out of these algorithms, superior tracking performance is exhibited by ACUKF.

Case 8: Here another real-time signal data is taken from the experiment, where frequency of the signal changes from 10 to 6 Hz and then back to 10 Hz as shown in Fig. 11*a*. The frequency tracking performance of the filters is summarised in Table 4.

Figs. 11*b* and *c* show that ACUKF performs much better than the UKF in tracking the signal waveform accurately. Fig. 11*d* shows comparison of frequency estimation performance of all the three algorithms.

The results obtained for different algorithms for different case studies are summarised in Tables 1 and 2.

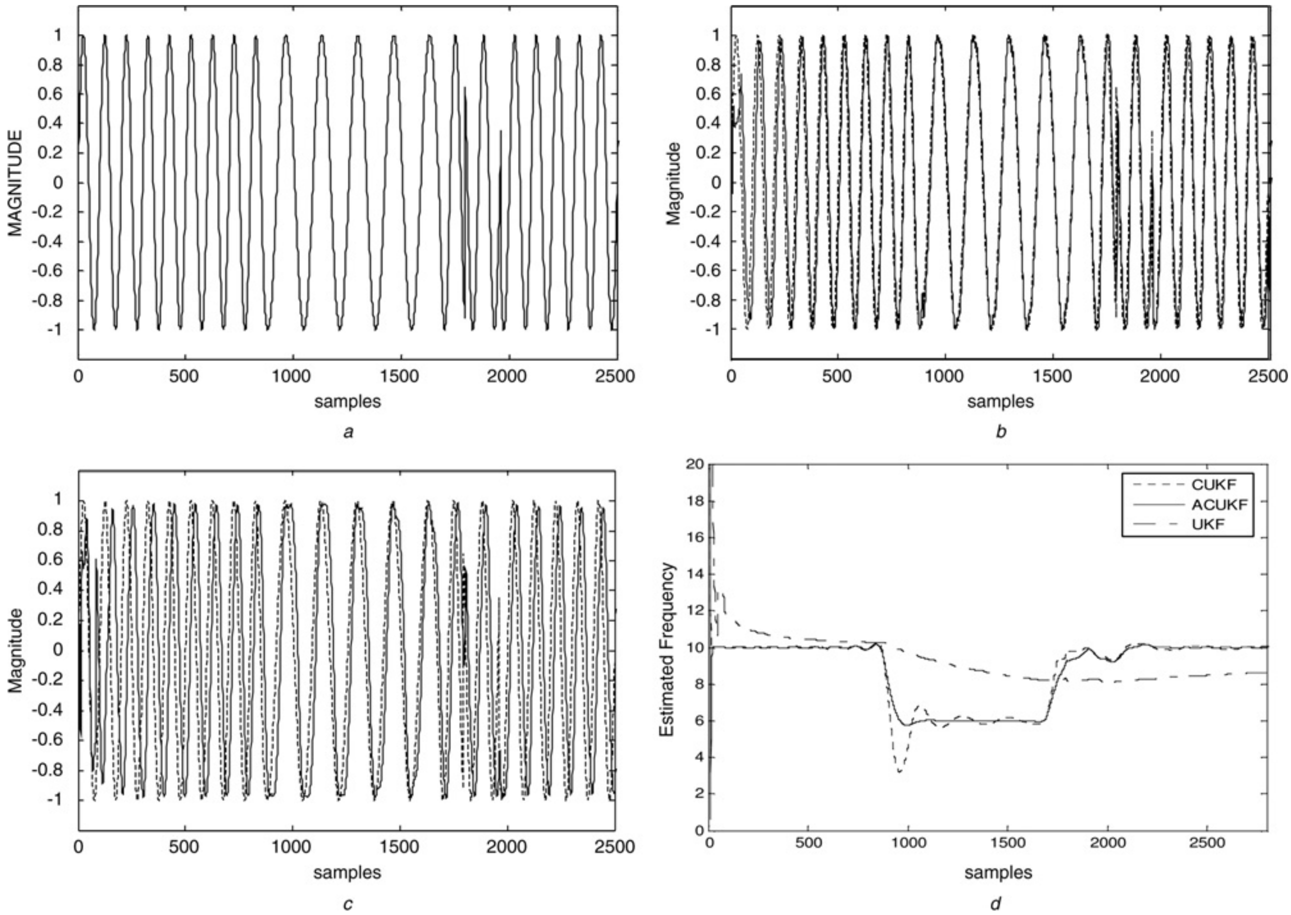

Figure 11 *Real-time signal tracking during frequency step-down*

a Real-time signal
b Real-time signal tracked using ACUKF: actual (dotted), estimated (solid)
c Real-time signal tracked using UKF algorithm: actual (dotted), estimated (solid)
d Real-time signal frequency tracked with different algorithms

doi: 10.1049/iet-smt.2009.0003

6 Conclusion

A non-linear filter based on UT and a complex state-space signal model (CUKF) has been proposed for the estimation of frequency of a time-varying sinusoid in the presence of high noise condition. The error performance of the proposed algorithm is analysed and the algorithm is modified for sequentially calculating the error covariance as a function of the sum of the absolute error values (ACUKF). Further, the stability analysis of the proposed non-linear filter has also been presented to prove its convergence property. It is observed that, the proper selection of $\hat{Q}_k$ is a tradeoff between stability and accuracy requirement of the filter. The proposed method is applied and compared with other algorithms for several simulation examples and real-time signals showing its superior performance.

7 References

[1] PHADKE A.G., THORP J.S., ADAMIAK M.: 'A new measurement technique for tracking voltage phasors, local system frequency and rate of change of frequency', *IEEE Trans. Power Apparat. Syst.*, 1983, **102**, pp. 1025–1038

[2] SACHDEV M.S., GIRAY M.M.: 'A least square technique for determining power system frequency', *IEEE Trans. Power Appar.. Syst.*, 1985, **104**, pp. 437–443

[3] HANDEL P., NEHORAI A.: 'Tracking analysis of an adaptive notch filter with constrained poles and zeros', *IEEE Trans. Signal Process.*, 1994, **42**, (2), pp. 281–291

[4] TICHAVSKY P., HANDEL P.: 'Two algorithms for adaptive retrieval of slowly time varying multiple cissoids in noise', *IEEE Trans. Signal Process.*, 1995, **43**, (5), pp. 1116–1127

[5] TICHAVSKY P., NEHORAI A.: 'Comparative study of four adaptive frequency trackers', *IEEE Trans. Signal Process.*, 1997, **45**, (6), pp. 1473–1484

[6] HANDEL P., TICHAVSKY P., SAVARESI S.M.: 'Large error recovery for a class of frequency tracking algorithms', *Int. J. Adapt. Control Signal Process.*, 1998, **12**, pp. 417–436

[7] TERZIJA V.V., DJRIC M.B., KOVACEVIC B.D.: 'Voltage phasor and local system frequency estimation using Newton-type algorithms', *IEEE Trans. Power Deliv.*, 1994, **4**, pp. 1368–1374

[8] TERZIJA V.V.: 'Improved recursive newton-type algorithm for frequency and spectra estimation in power systems', *IEEE Trans. Instrum. Meas.*, 2003, **52**, (5), pp. 1654–1659

[9] YANG J., XI H., GUO W.: 'Robust modified Newton algorithm for adaptive frequency estimation', *IEEE Signal Process. Lett.*, 2007, **14**, (11), pp. 879–882

[10] LA SCALA B.F., BITMEAD R.R.: 'Design of an extended Kalman filter frequency tracker', *IEEE Trans. Signal Process.*, 1996, **44**, (3), pp. 739–743

[11] LA SCALA B.F., BITMEAD R.R., QUINN B.G.: 'An extended Kalman filter frequency tracker for high-noise environments', *IEEE Trans. Signal Process.*, 1996, **44**, (2), pp. 431–434

[12] ROUTRAY A., PRADHAN A.K., PRAHALLAD RAO K.: 'A novel Kalman filter for frequency estimation of distorted signals in power systems', *IEEE Trans. Instrum. Meas.*, 2002, **51**, (3), pp. 469–479

[13] XIONG K., ZHANG H., LIU L.: 'Adaptive robust extended Kalman filter for nonlinear stochastic systems', *IET Control Theory Appl.*, 2008, **2**, (3), pp. 239–250

[14] JULIER S., UHLMANN J., DURRANT-WHYTE H.F.: 'A new method for the nonlinear transformation of means and covariances in filtering and estimators', *IEEE Trans. Autom. Control*, 2000, **45**, pp. 477–482

[15] ROMANENKO A., CASTRO J.A.A.M.: 'The unscented filter as an alternative to the EKF for nonlinear state estimation: a simulation case study', *Comput. Chem. Eng.*, 2004, **28**, pp. 347–355

[16] XIONG K., ZHANG H.Y., CHAN C.W.: 'Performance evaluation of UKF-based nonlinear filtering', *Automatica*, 2006, **42**, pp. 261–270

[17] NISHIYAMA K.: 'A nonlinear filter for estimating a sinusoidal signal and its parameters in white noise: on the case of a signal sinusoid', *IEEE Trans. Signal Process.*, 1997, **45**, pp. 970–981

[18] DASH P.K., PRADHAN A.K., PANDA G.: 'Frequency estimation of distorted power system signals using extended complex Kalman filter', *IEEE Trans. Power Deliv.*, 1999, **14**, (3), pp. 761–766

[19] ABDEL-GALIL T.K., EL-SAADANY E.F., SALAMA M.M.A.: 'Online tracking of voltage flicker utilizing energy operator and Hilbert transform', *IEEE Trans. Power Deliv.*, 2004, **19**, (2), pp. 861–867